Received: 13 June 2022 | Revised: 20 July 2022 | Accepted: 3 August 2022

DOI: 10.1111/dgd.12809

RESEARCH ARTICLE

Development, Growth & Differentiation WILEY

A PI3Kγ signal regulates macrophage recruitment to injured tissue for regenerative cell survival

Siyu Zhou | **Zhengcheng Liu** | **Atsushi Kawakami**

School of Life Science and Technology, Tokyo Institute of Technology, Yokohama, Japan

Correspondence
Atsushi Kawakami, School of Life Science and Technology, Tokyo Institute of Technology, B27, 4259 Nagatsuta, Midori-ku, Yokohama 226-8501, Japan.
Email: atkawaka@bio.titech.ac.jp

Funding information
Challenging Exploratory Research, Grant/Award Number: 19K22417; Grant-in-Aid for Scientific Research (B), Grant/Award Number: 19H03232

Communicating Editor: Yasuhiro Kamei

Abstract

The interaction between immune cells and injured tissues is crucial for regeneration. Previous studies have shown that macrophages attenuate inflammation caused by injuries to support the survival of primed regenerative cells. Macrophage loss in zebrafish mutants like *cloche* (*clo*) causes extensive apoptosis in the regenerative cells of the amputated larval fin fold. However, the mechanism of interaction between macrophage and injured tissue is poorly understood. Here, we show that a phosphoinositide 3-kinase gamma (PI3Kγ)-mediated signal is essential for recruiting macrophages to the injured tissue. PI3Kγ inhibition by the PI3Kγ-specific inhibitor, 5-quinoxalin-6-ylmethylene-thiazolidine-2,4-dione (AS605240 or AS), displayed a similar apoptosis phenotype with that observed in *clo* mutants. We further show that PI3Kγ function during the early regenerative stage is necessary for macrophage recruitment to the injured site. Additionally, protein kinase B (Akt) overexpression in the AS-treated larvae suggested that Akt is not the direct downstream mediator of PI3Kγ for macrophage recruitment, while it independently plays a role for the survival of regenerative cells. Together, our study reveals that PI3Kγ plays a role for recruiting macrophages in response to regeneration.

KEYWORDS
apoptosis, macrophage, PI3K, regeneration, zebrafish

1 | INTRODUCTION

Tissue homeostasis including regeneration and cellular turnover is crucial for maintaining tissue integrity of multicellular organisms. Mammals have a limited capacity to restore the lost tissue; however, some vertebrate species such as urodele amphibians and teleost fish retain a high regeneration potential. Dissecting the regeneration mechanism in such model species may contribute to the development of new regenerative therapies.

Zebrafish possesses a remarkable capacity to regenerate a variety of tissues, including appendages like fins, eyes, heart, spinal cord, and many other organs throughout their lifespan. Like the limb regeneration in urodeles, the fish fin regenerates through a process called as epimorphic regeneration that includes the formation of characteristic tissues like the wound epidermis (WE) and blastema (Kawakami, 2010; Poss et al., 2003). Using the adult zebrafish caudal fin as a model, the molecular basis has been explored during the past decade to reveal necessary roles of multiple signaling pathways such as Fgf, Hedgehog, and Wnt signaling during regeneration (Poss, 2010; Wehner & Weidinger, 2015).

In addition to the adult fin, the zebrafish larval fin fold was also used as a regeneration model to dissect the underlying molecular

mechanism (Kawakami et al., 2004; Mateus et al., 2012; Yoshinari & Kawakami, 2011). The neuregulin (NRG) and ErbB signaling was shown to be necessary for cell proliferation and migration during zebrafish fin fold regeneration (Rojas-Muñoz et al., 2009). Further, it has also been shown that phosphorylation of Junb family proteins is required for cell cycle activation and a proper regeneration progress (Ishida et al., 2010). Thus, increasing numbers of studies using the larval fin fold model have contributed for revealing the molecular basis of regeneration (Kawakami, 2010; Yoshinari & Kawakami, 2011).

Recently, several studies have suggested that immune cells like macrophages and their inflammatory response play crucial roles for tissue regeneration in zebrafish and other species (Aztekin et al., 2020; Simões et al., 2020). Activated macrophages eliminate senescent cells to support salamander limb regeneration and prevent tissue aging (Yun et al., 2015). In addition, macrophages contribute to salamander tissue regeneration by controlling inflammatory actions and cytokine signaling (Godwin et al., 2013). Further, it has been shown that genetic ablation of macrophages in adult zebrafish impairs bony ray formation during caudal fin regeneration (Petrie et al., 2014). Moreover, macrophages also control zebrafish spinal cord regeneration through modulation of a proinflammatory cytokine, *interleukin-1β* (*il1b*), and a pro-regenerative cytokine, *tumor necrosis factor alpha* (*tnf-α*) (Tsarouchas et al., 2018).

Our preceding studies showed that macrophages are necessary for the survival of regenerative cells that are primed to initiate regeneration-induced gene expression and cell proliferation (Hasegawa et al., 2015 and 2017). We found that aberrant apoptosis in amputated fin folds and a regeneration defect occur in the amputated fin fold of the *cloche* (*clo*) mutant (Stainier et al., 1995) and other mutants in which hematopoietic cell development is defective (Hasegawa et al., 2015). We revealed that the apoptosis of regenerative cells is induced by prolonged and excess expression of *il1b* (Hasegawa et al., 2017), and that a factor, possibly derived from the macrophage, is responsible for attenuating inflammation and preventing the apoptosis of regenerative cells (Hasegawa et al., 2015). However, the molecular mechanisms and signals from the wounded tissue to macrophages and regenerative cell survival are not well understood.

This study aimed to determine the mechanism underlying the survival of regenerative cells by screening a chemical library. We found that the phosphoinositide 3-kinase gamma (PI3Kγ)-specific inhibitor (AS605240, written AS hereafter) induced apoptosis in tissues adjacent to the amputated site. From analyses of the effect of AS, we showed that PI3Kγ plays a role for recruiting macrophages to the injured tissue in response to injury.

2 | MATERIALS AND METHODS

2.1 | Zebrafish

The wild-type zebrafish strain used in this study was originally derived from the Tubingen strain and was maintained in our facility for over 10 years by inbreeding. Transgenic (Tg) strains used in this study are *Tg* (*mpeg1:mCherry*) (Ellett et al., 2011), *Tg*(*fn1b:egfp*) (Shibata et al., 2018), and *Tg*(*hsp70l:mKO2-t2a-caAkt*) (this study). All fish were maintained in a recirculating water system in a 14 h day/10 h night photoperiod at 28.5°C. Zebrafish larvae (2–4 days post fertilization, dpf) and adult fish (3–12 months old) with similar sex ratios were analyzed for all experiments unless otherwise specified. All surgery was performed under 0.002% tricaine (3-aminobenzoic acid ethyl ester, Sigma-Aldrich) anesthesia and every effort was made to minimize suffering. Animal experimentation was performed in strict accordance with the recommendations of the Act on Welfare Management of Animals in Japan, the Guide for the Care, Use of Laboratory Animals of the National Institute of Health, and the Animal Research Guidelines at Tokyo Institute of Technology, Japan. Experiments performed in accordance with the approved protocols complied with ARRIVE guidelines.

2.2 | Fin fold amputation

Adult fin regeneration experiments were performed on 3- to 12-month-old male zebrafish. The fish were anesthetized with tricaine and the caudal fins were cut in a straight line in the middle of the central fin ray. Fin regeneration was quantified by measuring the length from the amputation plane to the posterior tip of the fin.

For fin fold amputation, zebrafish larvae at 3 dpf were anesthetized with tricaine in egg water (0.006% artificial sea salt, 0.0001% methylene blue). Fin folds were cut with a scalpel at the site immediately posterior to the notochord end. The amputated fish were incubated in fresh egg water at 28.5°C, and the regenerating fins and fin fold were collected at appropriate time points for further analysis. The length from the notochord end to the posterior tip of the fin fold were measured to quantify fin fold regeneration.

2.3 | Generation of the transgenic line *Tg(hsp70l:mKO2-t2a-caAkt)*

The *pT2(hsp70l:mKO2-t2a-caAkt)* construct was prepared by inserting the *caAkt* cassette into *pT2(hsp70l:mKO2)* (Akieda et al., 2019). The 14-amino acid *src* myristoylation signal (Kohn et al., 1996) was fused to the zebrafish *Akt* sequence and the caAkt was placed under the control of the *heat shock protein 70 L* promoter. The engineered construct was injected into one-cell-stage zebrafish embryos with 25 ng/μL transposase mRNA. F0 founders were either incrossed or outcrossed to screen the F1 careers. The carriers were identified by mKO2 fluorescence after heat shock at 38°C for 2 h at 72 hpf.

2.4 | Chemical library screening

The library of 3404 compounds (LOPAC Validated A and B, Sigma Aldrich) were provided by the Tokyo University Drug Discovery

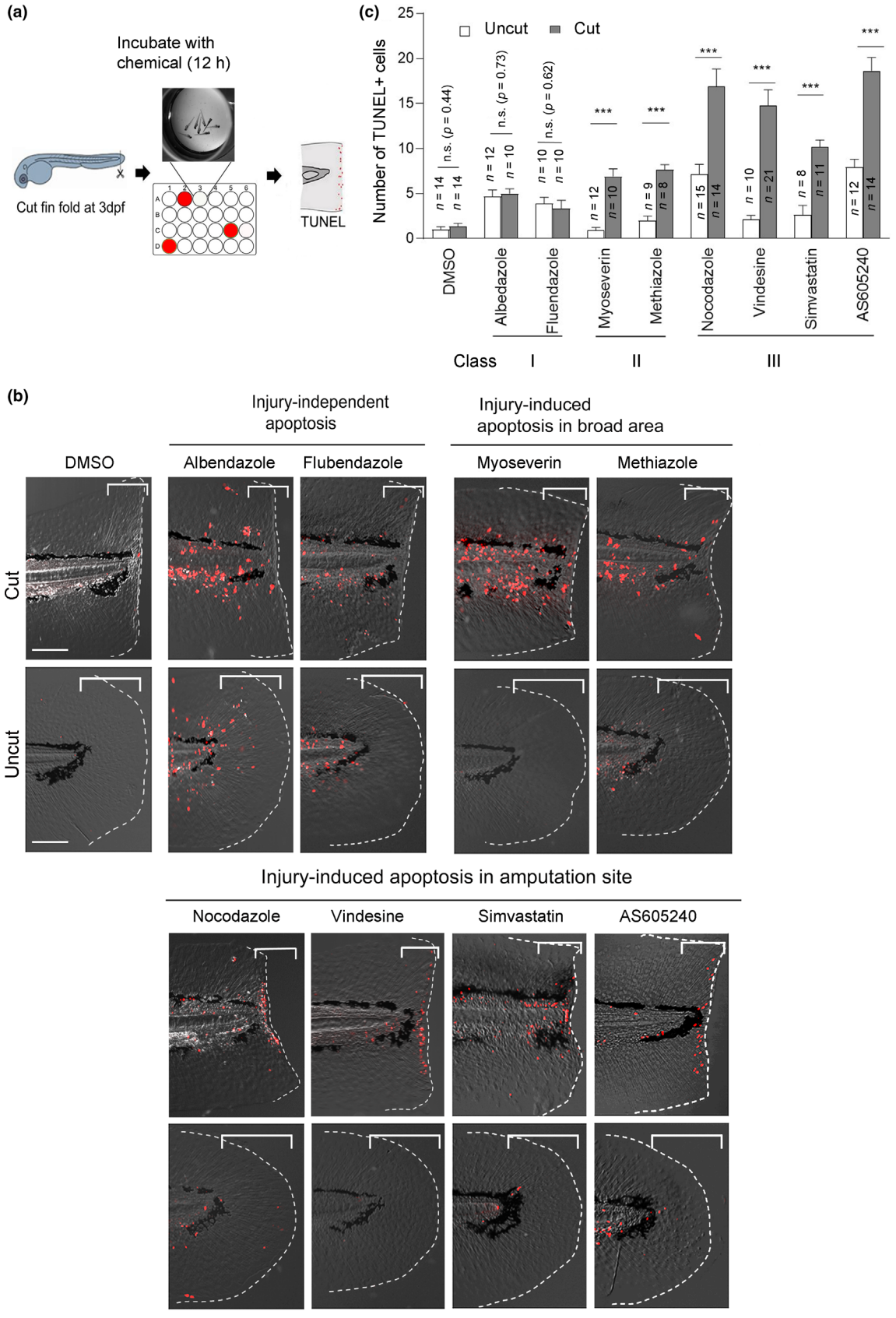

FIGURE 1 Legend on next page.

Initiative. The compounds were divided into 344 pools that contained 6–10 chemicals; most of the pools contained 10 chemicals. The chemical pools (1 mM each compound) were diluted 5-fold using DMSO and a further 200-fold with 1 ml egg water to a final concentration of 1 μM for each chemical and 0.5% DMSO. The chemicals were blind-tested and screened in 24-well plates with zebrafish larvae by incubating the larvae at 28.5°C for 12 hours. Apoptosis was detected by the terminal deoxynucleotidyl transferase dUTP nick end labeling (TUNEL). The first screen showed that 49 out of 344 pools (14.2%) were severely toxic and caused larval death within 12 h of incubation. These toxic pools were discarded and the individual chemicals were not further tested. The individual chemicals in the pools that displayed apparent apoptosis were successively screened and further validated.

All candidate chemicals were tested more than twice to confirm the phenotypes at 1 μM. However, AS (Selleck Chemicals) was used at 2 μM for further analysis of the larvae fin fold phenotype and 2.5 μM for the adult fin phenotype. AS was dissolved in DMSO at 10 mM and stored at −30°C. The stock was diluted to the working concentration with egg water and applied to zebrafish larvae in a 6-well plate at least 1 h before fin fold amputation.

2.5 | Morpholino (MO) injection

MOs obtained from Gene Tools were dissolved in Danieau solution at 1 mM, and injected (0.5 nL/egg) into the dechorionated fertilized zebrafish eggs at the 1–2 cell stage. The following MOs were used in this study:

pik3cg MO: 5′-CTGGCTTGCTGTTCCATAACCAATG-3′

pik3cg splice MO: 5′-GCTCAATCTGAAATTAAAATGGTGC-3′

std MO: 5′-CCTCTTACCTCAGTTACAATTTATA-3′.

pik3cg splice MO interferes with *pik3cg* RNA splicing to create a premature stop codon. A decrease in the *pik3cg* transcript caused by nonsense-mediated mRNA decay was confirmed using RT-PCR analysis (Figure 3a). The fluorescein-tagged ATG MO targets the translation initiation site (custom design by Gene Tools); this was used to confirm injection efficiency and the MO phenotype.

2.6 | RT-PCR analysis

RT-PCR was performed as described previously (Hasegawa et al., 2017). Total RNA was extracted from larval tail tissue (30 per group) posterior to the yolk extension using TRIzol (Thermo Fisher Scientific) and further purified using the RNeasy kit (Qiagen). cDNAs were synthesized using the Thermoscript RT-PCR kit (Thermo Fisher Scientific) with random hexamer as the primer. PCR was performed according to a standard procedure using Paq5000 DNA polymerase (Agilent Technologies) and the following primers:

pik3cg Fw: 5′-GTCTTAGGGTTGCCAGACAGCTTTAAAGTGCC-3′

pik3cg Rv: 5′- CTGAATGTTTGCAATGGTAGTGGCATCCTTC-3′

actb1 Fw: 5′-ATGAGGAAATCGCTGCCCTGGTCG-3′

actb1 Rv: 5′-ACCGTGCTCAATGGGGTATTTGAGGGT-3′.

2.7 | Time-lapse analysis of macrophage migration

For live imaging of *Tg*(*mpeg1:mCherry*), larvae were anesthetized with 0.002% tricaine, placed on a 2% agarose gel, embedded in 1.2% low melting-point agarose gel, and observed under a 20× water-immersion objective lens using a confocal laser scanning microscope (FV-1000, Olympus). Images were acquired once every 3 min to draw the movement trajectories of *mpeg1*$^+$ cells. The velocity of *mpeg1*$^+$ cells was analyzed using NIH ImageJ 1.49 and Microsoft Excel 2013.

2.8 | Histological analysis

Antibody staining was performed as previously described (Shibata et al., 2016) using 1:50 anti-rabbit phospho-Akt (pAKT) (Ser473) antibody (#4060, Cell Signaling Technology) and 1:250 goat anti-rabbit Alexa Fluor 568 antibody (#A-11011, Invitrogen). The stained samples were mounted with 80% glycerol containing 25 mg/mL triethylenediamine (DABCO, Nacalai Tesque) as an anti-fading reagent. Immunostained larvae were observed with the FA6000 fluorescent stereomicroscope (Leica).

Cell proliferation was detected by 5-ethynyl-2′-deoxyuridine (EdU) incorporation using the Click-iT EdU imaging kit (Life Technologies) as previously described (Shibata et al., 2018). Zebrafish larvae and adults were incubated in egg water containing EdU (1 mM for larvae and 50 μM for adult fin) for 24 h at 28.5°C. EdU detection was performed according to the manufacturer's instructions. The samples were mounted with 80% glycerol containing DABCO. The EdU-positive cells were quantified by captured images.

Cell apoptosis was detected by TUNEL staining using the in situ apoptosis detection kit (Roche) as previously described (Hasegawa

FIGURE 1 Screening compounds that induce apoptosis in the larvae fin fold. (a) Schematic overview of the screening procedure. Wild type (WT) zebrafish larvae were amputated at 3 days post fertilization (dpf) and incubated with the compounds for 12 h in a 24-well plate. Uncut larvae were also incubated as a control. Apoptotic effects were evaluated by TUNEL (terminal deoxynucleotidyl transferase dUTP nick end labeling) staining. (b) Representative apoptosis phenotypes caused by the respective chemicals. Class I compounds (albendazole and flubendazole) induced ubiquitous apoptosis in cut and uncut larvae. Class II and III compounds induced apoptosis in response to tissue amputation. Class III compounds (nocodazole, vindesine, simvastatin, and AS605240), induced apoptosis mostly close to the amputation site, whereas class II compounds (myoseverin and methiazole) induced apoptosis in broader areas. Scale bar, 50 μm. (c) Quantification of the number of apoptotic cells in the bracketed areas from the posterior end of the notochord to the amputation plane in (b). Data are presented as the mean ± SEM. Student's *t*-test. ***$p < 0.001$. n.s., not significant. DMSO, dimethyl sulfoxide

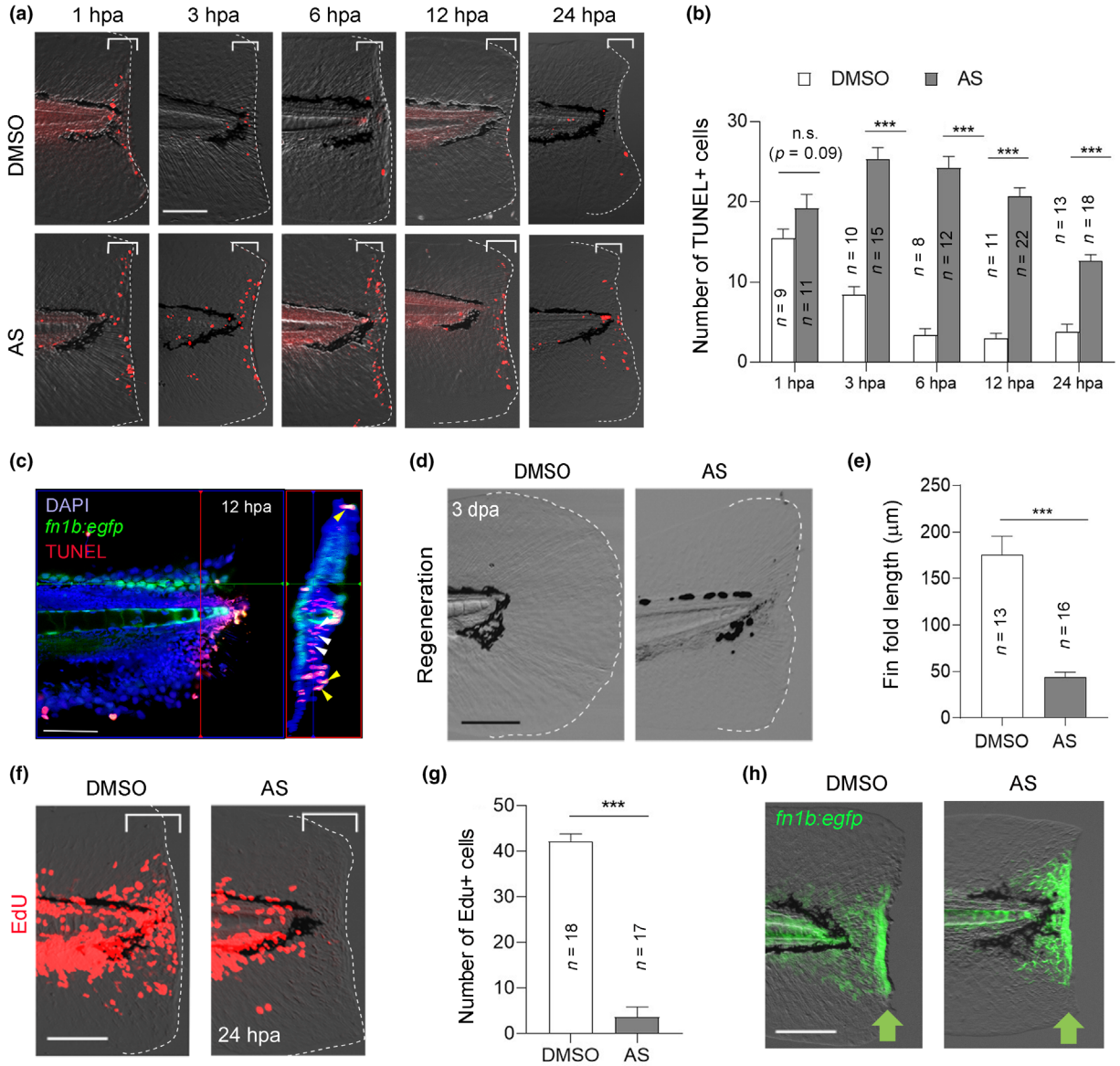

FIGURE 2 Phenotype caused by the PI3Kγ inhibitor, AS. (a) Terminal deoxynucleotidyl transferase dUTP nick end labeling (TUNEL) analysis of cell death at different stages of fin fold regeneration using dimethyl sulfoxide (DMSO)- and AS-treated larvae. Scale bar, 50 μm. (b) Quantification of TUNEL-positive cells in the injured site (bracketed areas) in (a). The data at 12 hpa (hours post amputation) in Figure 1b were also used for statistical analysis. (c) Confocal image of the fin fold of *Tg(fn1b:egfp)* (green) at 12 hpa wherein apoptotic cells were detected by TUNEL staining (red). Right panel, the longitudinal transverse optical section at a plane indicated by the red line. DAPI, nuclear staining with 4′,6-diamidino-2-phenylindole dihydrochloride (0.1 mg/mL). The enhanced green fluorescent protein (EGFP) fluorescence marks the epithelial cells expressing *fn1b*. Yellow and white arrowheads indicate representative epithelial and mesenchymal cells, respectively. Scale bar, 50 μm. (d) Fin fold regeneration in DMSO- and AS-treated larvae at 3 dpa. Scale bar, 50 μm. (e) Quantification of the regenerated fin fold length from the posterior to the end of notochord in (d). (f) Detection of proliferating cells by 5-ethynyl l-2′-deoxyuridine (EdU) incorporation in the DMSO- and AS-treated larvae during 0–24 hpa. Scale bar, 50 μm. (g) Quantification of the number of EdU-positive cells beneath the amputation site (bracketed areas) in (f). (h) Confocal image of the fin fold of *Tg(fn1b:egfp)* at 12 hpa in the DMSO- and AS-treated larvae. Scale bar, 50 μm. (b, e, g) Data are presented as the mean ± SEM and analyzed by Student's *t*-test; ***$p < 0.001$, n.s., not significant

et al., 2017). The posterior tissue containing the larval tail was cut and reacted with TUNEL reaction mixture at 37°C for 2 h. The samples were mounted with 80% glycerol containing DABCO, and the images were acquired with the FA6000 fluorescent stereomicroscope (Leica), LSM780 confocal microscope (Zeiss), or FV1000 (Olympus) confocal laser-scanning microscope.

2.9 | Quantification and statistical analysis

Clutchmates were randomized into different treatment groups for each experiment. No animal or sample was excluded from the analysis unless the animal died during the procedure. All experiments were performed with at least three biological replicates unless

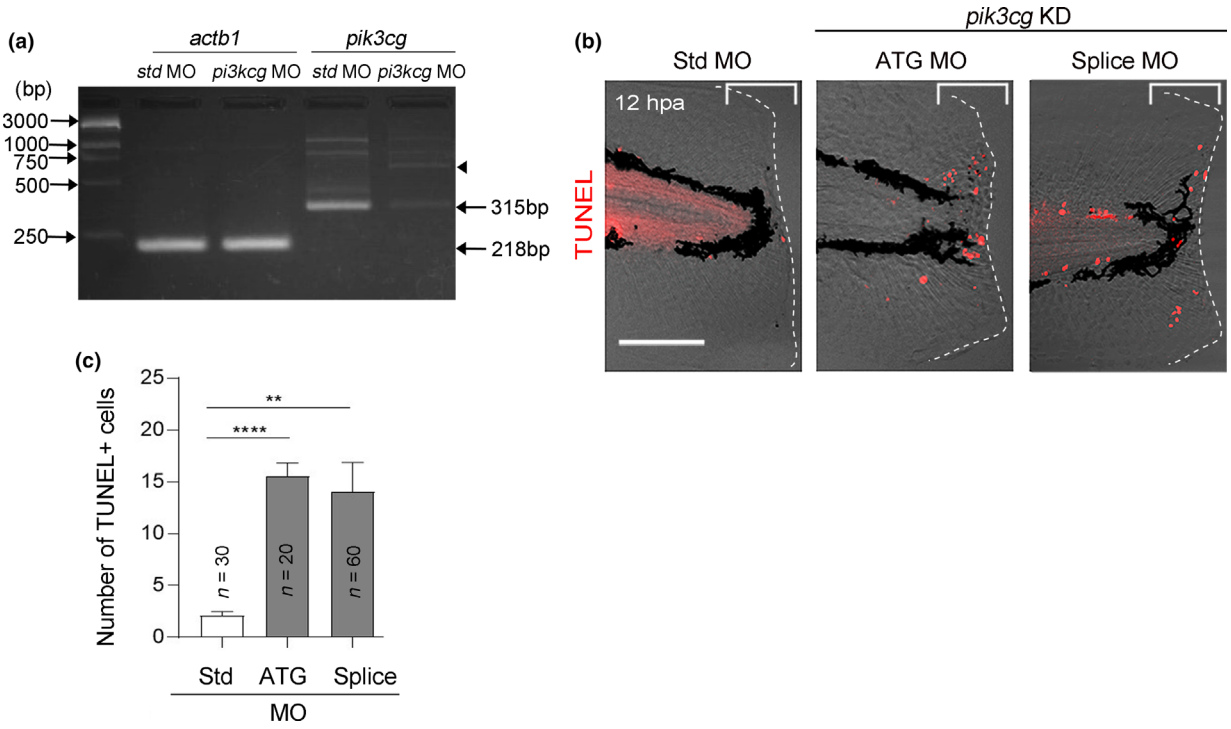

FIGURE 3 *Pik3cg* knockdown recapitulates the phenotypes in AS-treated larvae. (a) RT-PCR analysis of *pik3cg* mRNA expression in larvae injected with standard control (std) morpholino (MO) or splice site MO. Blocking mRNA splicing causes a premature stop codon and induces mRNA degradation. Arrowhead indicates a minor 750-bp PCR product that may be derived from unspliced mRNA. (b) Terminal deoxynucleotidyl transferase dUTP nick end labeling (TUNEL) analysis of larvae injected with std-, ATG-, or splice MOs at 12 hpa. Scale bar, 50 μm. (c) Quantification of TUNEL-positive cells in the injured site (bracket region) in (b). Statistical significance was tested by one-way ANOVA; $^{**}p < 0.05$, $^{***}p < 0.001$

otherwise stated using the appropriate number of samples for each replicate. Sample sizes were chosen based on those reported in previous publications and experiment types and are indicated in each figure legend. Statistical analyzes were performed using Microsoft Excel 2013 or IBM SPSS software. All statistical values are displayed as the mean ± standard error of the mean. Sample sizes, statistical tests, and *p* values are indicated in the figures or legends. Student's *t*-tests (two-tailed) or the ANOVA test for statistical significance were applied when normality and equal variance tests were passed. The ANOVA test was used for three or more groups of data.

The *mpeg1*$^{+}$ cells in the ventral region of the tail between the caudal artery and cardinal vein were counted for quantification of *mpeg1*$^{+}$ cells in the caudal hematopoietic tissue (CHT) region. Quantification of apoptotic cells involved counting TUNEL-positive nuclei in the captured and enlarged images. Quantification of EdU incorporation in the adult fin and pAkt staining in the larval fin fold involved capturing fluorescent images using a Leica FA6000 microscope with a DFC365Fx B/W camera and LAS X software (Ver. 3.7.0) under the same non-saturated conditions. The acquired fluorescent images were binarized at a fixed condition for each experiment using NIH ImageJ 1.49 to quantify the fluorescence. Fluorescence was measured by applying a color threshold (red–green–blue color model) to select only the areas appearing in red. Pixel measurements were converted into units of area.

3 | RESULTS

3.1 | Screening for apoptosis-inducing compounds

To obtain a clue for the mechanisms how the survival and maintenance of regenerative cells are regulated, a chemical library was screened by TUNEL analysis for compounds that induce apoptosis during zebrafish larval fin fold regeneration (Figure 1a). An initial screen using pools of chemicals (344 pools, 6–10 chemicals/pool) identified 26 pools that displayed increased apoptosis in the amputated fin fold at 12 h post amputation (hpa). The individual compounds were further screened to finally identify eight compounds that significantly increased apoptosis.

The identified compounds were grouped into three classes (Figure 1b,c). Class I compounds including albendazole and flubendazole caused apoptosis irrespective of amputation (Figure 1b). These drugs are known as antiparasitic drugs that bind to tubulin to suppress microtubule polymerization (Geary et al., 2019). They are also shown to induce p53-mediated apoptosis and arrest the cell cycle at the G2/M phase in rat embryos (Longo et al., 2013; Longo et al., 2014).

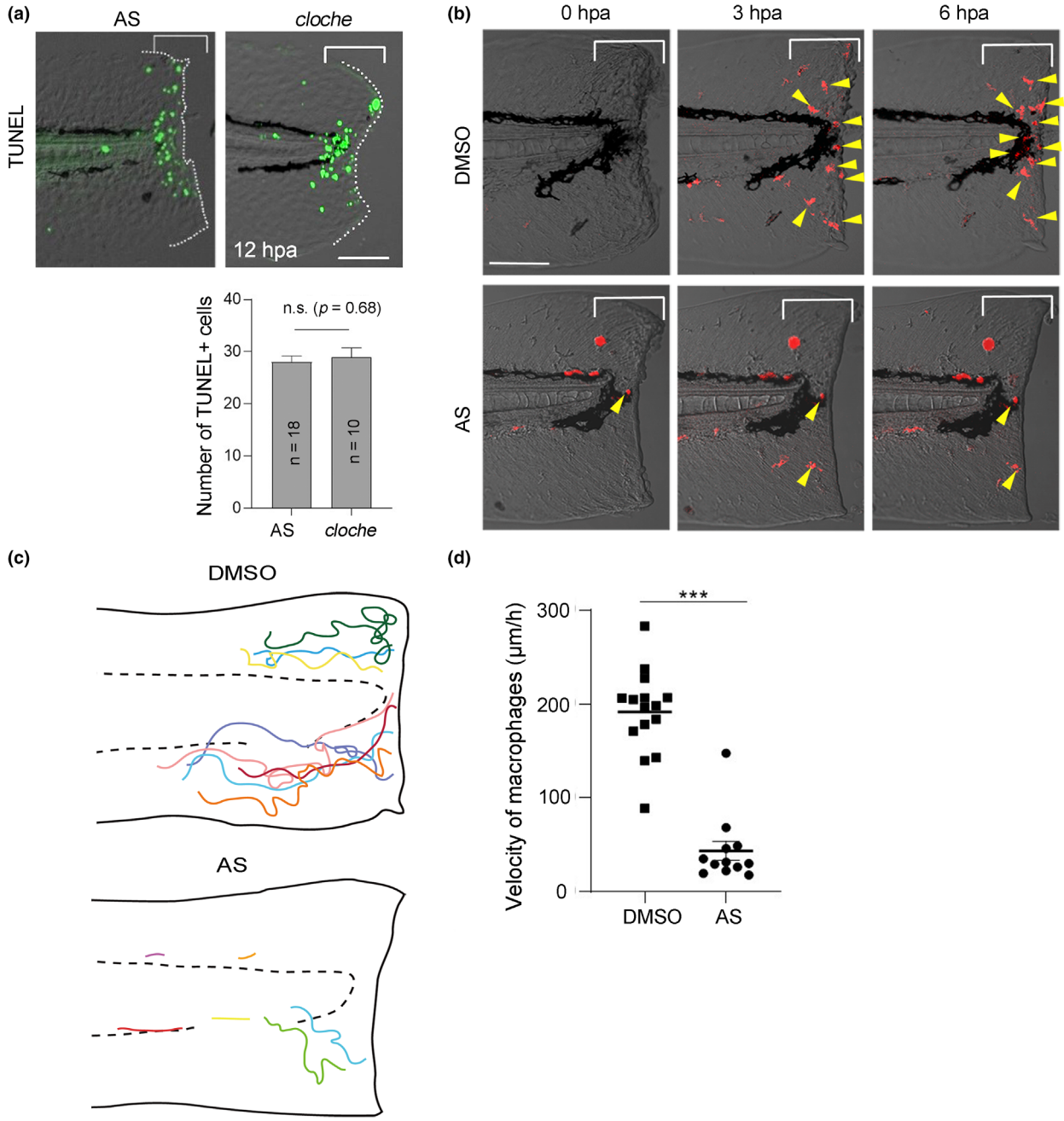

FIGURE 4 Loss of macrophage recruitment caused by PI3Kγ knockdown. (a) Comparison of regeneration-dependent apoptosis of AS-treated larva and *cloche* (*clo*) mutant. Terminal deoxynucleotidyl transferase dUTP nick end labeling (TUNEL) stained AS-treated larva and *clo* mutant was compared side-by-side at 12 hpa. Scale bar, 50 μm. (b) Macrophage migration and accumulation at the injured site visualized by *Tg*(*mpeg1:mCherry*). The time-lapse recording was done at 0–6 hpa with a confocal microscope using a water immersion objective lens, and the images were taken from the recorded live images. Yellow arrowheads indicate *mpeg1*$^{+}$ macrophages. Scale bar, 50 μm. (c) Schematic diagrams showing a 6 h time-lapse of the injured fin fold and migration trajectory of macrophages arriving at the wound in dimethyl sulfoxide (DMSO)- and AS-treated larvae during the recruitment phase. Respective colored lines indicate the trajectories of individual macrophages. (d) Macrophage velocity quantification in DMSO- and AS-treated larvae. Data are presented as the mean ± SEM and analyzed by Student's *t*-test; ***$p < 0.001$. For further information, please refer to Videos S1 and S2

Class II compounds including myoseverin and methiazole displayed injury-induced apoptosis in a broad area away from the amputated site (Figure 1b). Myoseverin is a microtubule-binding molecule and an inhibitor of tubulin polymerization (Rosania et al., 2000), while methiazole is used as a medication for hyperthyroidism by inhibiting thyroid hormone synthesis (Nakamura et al., 2007). It has been reported that myoseverin and methiazole induce apoptosis in mammalian mononuclear myotube cells (Um et al., 2017) and the rat olfactory neurons through caspase 3 activation (Sakamoto et al., 2007).

Class III compounds including nocodazole, vindesin, simvastatin, and AS, increased apoptosis in the area close to the injured site (Figure 1b). Nocodazole and vindesin are microtubule de-polymerizing agents and

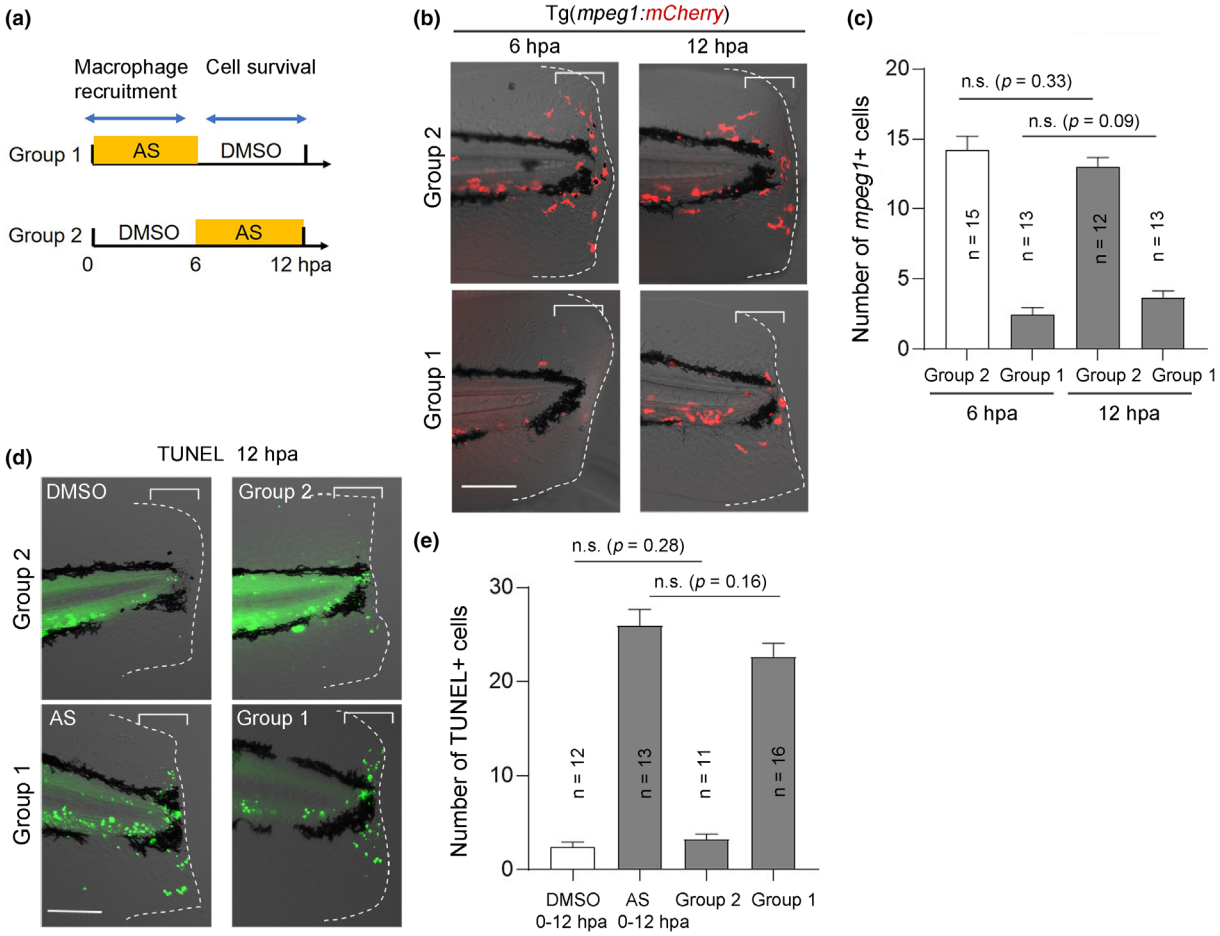

FIGURE 5 PI3Kγ function is required during the early stages of fin fold regeneration. (a) The experimental scheme of stage-specific treatment of AS. Group 1 larvae were exposed to AS 0–6 hpa to block macrophage recruitment. Group 2 larvae were exposed to AS 6–12 hpa to allow macrophage recruitment. (b) Macrophage recruitment detected using *Tg(mpeg1:mCherry)* at 6 and 12 hpa. Macrophages accumulated in the injured site of only group 2 larvae. Scale bar, 50 μm. (c) Quantification of the number of *mpeg1*$^{+}$ cells in the injured site (bracket areas) in (b). (d) Terminal deoxynucleotidyl transferase dUTP nick end labeling (TUNEL) analysis of two larval groups at 12 hpa. Scale bar, 50 μm. (e) Quantification of the number of TUNEL-positive cells in the injured site (bracket areas) in (d). (c and e) Data are presented as the mean ± SEM. Statistical significance was analyzed using one-way ANOVA. n.s., not significant

induce cell death by arresting the cell cycle (Frank et al., 2019; Merighi et al., 2003). Statins such as simvastatin inhibit 3-hydroxy-3-methylglutaryl-coenzyme A reductase, a rate-limiting enzyme in the mevalonate pathway for cholesterol synthesis (Todd & Karen, 1990). AS is an ATP-competitive inhibitor against phosphoinositide 3-kinase gamma (PI3Kγ) (Camps et al., 2005). The following section investigated the action of the AS during fin fold and fin regeneration.

3.2 | Phenotypes caused by PI3Kγ inhibition

TUNEL analysis was performed at different regenerative stages to further characterize AS-mediated apoptosis. Many apoptotic cells were detected at 1 hpa in both (DMSO)- and AS-treated larvae (Figure 2a) due to cell destruction by amputation (Hasegawa et al., 2015). However, apoptosis remained high only in AS-treated larvae during 3–12 hpa and gradually declined thereafter (Figure 2a,b), indicating that AS-specific apoptosis occurs in stages from 3 hpa onwards. Confocal optical sections showed that higher apoptosis occurred in mesenchymal cells, although a low-level apoptosis also occurred in epithelial cells (Figure 2c). In addition, AS impaired tissue regeneration (Figure 2d,e) and cell proliferation (Figure 2f,g), whereas AS did not affect the WE formation and the *fn1b* induction in the epithelial cells around the amputated site (Figure 2h).

We also validated if AS targets PI3Kγ during apoptosis. Two antisense morpholino oligonucleotides (MOs) were used to target the translation initiation site and the exon-intron boundary (Yoo et al., 2010), respectively, to knockdown the *pik3cg* gene encoding PI3Kγ (Figure 3a) and examine apoptosis in the morphants. Apoptosis around the amputation site increased in larvae injected with either of the *pik3cg* MOs in the same way as in the AS-treated larvae (Figure 3b,c), suggesting that PI3Kγ is at least the major driver for the apoptosis phenotype caused by AS. The number of apoptotic cells caused by the MO injection were slightly less than that of AS. This is possibly due to the lower penetrance of MOs at later developmental stages.

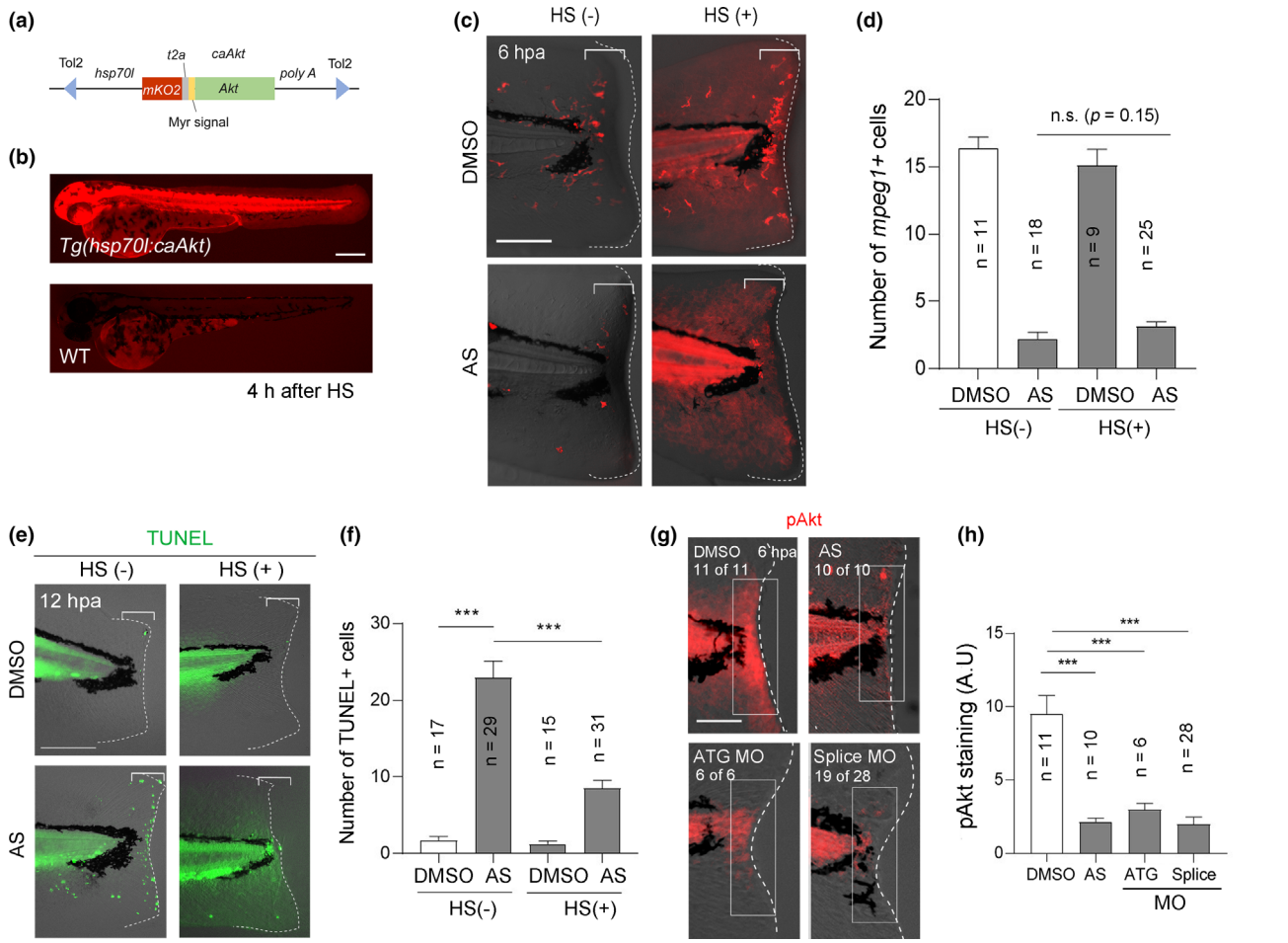

FIGURE 6 Akt functions in regenerative cells for their survival. (a) Schematic diagram of the overexpression construct. The zebrafish *hsp70l* promoter drives *mKO2* and *caAkt* expression. (b) Induction of mKO2 expression in the embryo (2 dpf) of the Tg line, *Tg(hsp70l:caAkt)*, after heat shock (HS). Scale bar, 250 μm. (c) TUNEL analysis at 12 hpa in the amputated fin fold with or without heat shock before amputation. Scale bar, 50 μm. (d) Quantification of the number of terminal deoxynucleotidyl transferase dUTP nick end labeling (TUNEL)-positive cells in the injured site (bracket areas) in (c). (e) Analysis of *mpeg1*$^{+}$ macrophage recruitment at 6 hpa in *Tg(hsp70l:caAkt)* with or without heat shock in the presence of dimethyl sulfoxide (DMSO) or AS. Scale bar, 50 μm. (f) Quantification of *mpeg1*$^{+}$ cells in the bracketed areas in (e). Akt overexpression did not rescue the AS-mediated defect in macrophage recruitment. (g) Immunostaining of phosphorylated Akt (pAkt, Ser 473) in DMSO- or AS-treated larvae, and in the *pik3cg* morphants injected with ATG or splice MOs. Scale bar, 50 μm. (h) Quantification of the fluorescent intensity of pAkt staining in the bracketed areas in (g) by measuring the fluorescent intensity in the boxed area (50 μm × 150 μm) by Image J. (d, f, h) Data are presented as the mean ± SEM. Statistical significance was analyzed by one-way ANOVA; ***$p < 0.001$; n.s., not significant

AS-treated regenerating adult fin and larval fin fold showed similar phenotypes in apoptosis, cell proliferation, and regeneration (Figure S1). This suggests that PI3Kγ is necessary for the survival of regenerative cells and regeneration during adult fin regeneration.

3.3 | PI3Kγ function is required for macrophage recruitment

We previously showed that the absence of macrophages (but not neutrophils) in the *clo* mutant caused apoptosis of regenerative cells (Hasegawa et al., 2015; Hasegawa et al., 2017). The phenotypes caused by AS treatment in this work were similar to those observed in the *clo* mutant (Hasegawa et al., 2017) (Figure 4a). We suspected that PI3Kγ inhibition could occur due to the abnormal macrophage behavior. Therefore, macrophages were tracked using *Tg(mpeg1:mCherry)* (Ellett et al., 2011) to investigate how AS impairs macrophage recruitment to the injured site. The *mpeg1*-expressing macrophage population accumulated at the injured site 3–6 hpa after fin fold amputation in the DMSO-treated control; however, they did not accumulate in AS-treated larvae (Figure 4b; Videos S1 and S2). Tracking of individual macrophages revealed that macrophage motility is severely impaired in the presence of the AS (Figure 4c,d). Macrophages in the AS-treated larvae have a rounder shape, while DMSO-treated macrophages have an irregular shape with many long filopodia. We further confirmed that the overall number of macrophages was unaffected by AS treatment. The number of macrophages in the CHT did not significantly decrease following AS treatment (Figure S2). Taken together, we concluded that AS

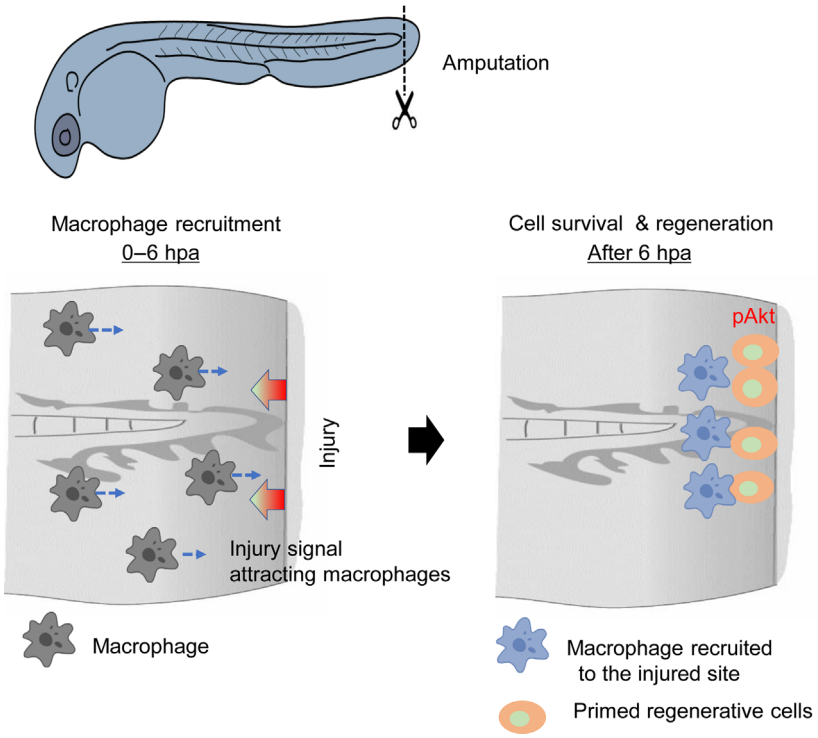

FIGURE 7 Summary of the roles of PI3Kγ for macrophage recruitment and survival of regenerative cells. The PI3Kγ-mediated signal regulates the recruitment of macrophages to the injured tissue during the early regenerative stage. The macrophages recruited to the wounded site provide a diffusible substance for regenerative cell survival. Phosphorylation of Akt (pAkt) induced by macrophage recruitment supports cell survival

treatment affected macrophage motility and their accumulation in the injured site and led to apoptosis of regenerative cells.

3.4 | PI3Kγ function is required during the early stages of regeneration

Many studies have suggested that PI3K signaling is involved in cell survival of many cellular systems (Franke et al., 2003). Therefore, it is possible that AS also has a direct effect on the survival of regenerative cells in the stage of macrophage recruitment. To test this possibility, the AS was applied at different time windows (group 1: 0–6 hpa; group 2: 6–12 hpa, where macrophage recruitment had already occurred) (Figure 5a). Macrophage recruitment was nearly completed by 6 hpa (Figure 5b,c). If AS acts on the injured site to induce apoptosis in a macrophage-independent manner, it is expected that apoptosis will increase in larvae treated with AS during 6–12 hpa.

However, the apoptosis level of group 1 larvae was almost the same with that of AS-treated during 0–12 hpa (Figure 5d,e). In contrast, no significant increase of apoptosis was observed in the larvae of group 2 (Figure 5d,e). These results suggest that PI3Kγ function is required before macrophage recruitment, and AS does not directly affect regenerative cell survival.

3.5 | Akt functions in the injured site to support their survival

It has been suggested that protein kinase Akt is the downstream mediator of the PI3K signal in many biological systems (Vara et al., 2004). To examine the possible involvement of Akt in the downstream of PI3Kγ, we generated the zebrafish Tg line that expresses the constitutively active form of Akt, *caAkt* (Kohn et al., 1996), under the control of *heat shock protein 70l* promotor (Figure 6a,b).

However, contrary to our expectation, we observed that the macrophage recruitment was not rescued by *caAkt* expression in the *Tg* after heat shock (Figure 6c and d), while AS-induced apoptosis significantly decreased despite the absence of macrophages (Figure 6e,f). These results suggest that Akt is not the downstream mediator for macrophage recruitment; instead, it functions independently in the surviving cells to support their subsistence.

To further investigate the site of Akt action, phosphorylated Akt (pAkt) immunostaining was performed. Apparent pAkt staining was observed in the injured tissue in response to injury (Figure 6g,h), while pAKt was severely decreased by AS treatment and *pik3cg* knockdown. These observations support the notion that Akt functions in the surviving cells.

4 | DISCUSSION

Through chemical library screening and functional analyzes, we revealed that PI3Kγ plays an essential role as a key signal for recruiting macrophages to the injured site in response to tissue injury. Additionally, we suggest that Akt is not the direct mediator of the PI3Kγ signal for macrophage recruitment (Figure 7).

Zebrafish is useful for large scale screening of chemicals that affects specific biological processes like tissue regeneration due to the ease of applying chemicals and observing phenotypes under the microscope (Han et al., 2019; Mishra et al., 2020;

Oppedal & Goldsmith, 2010). In particular, the larval stage is small enough to perform high-throughput screening (Mathew et al., 2007). We screened for compounds that induce aberrant cell death in the regenerating fin fold of zebrafish larvae and successfully identified eight apoptosis-inducing compounds from a library of >3000 compounds.

Further analysis of the PI3Kγ selective inhibitor (AS) in this work showed that PI3Kγ plays a crucial role for recruiting macrophages to the injured site to support the survival of regenerative cells. However, Akt could not rescue macrophage recruitment in the presence of AS, indicating that Akt is not the downstream mediator for macrophage recruitment. On the other hand, Akt rescued apoptosis caused by the loss of macrophages in the injured site, suggesting that the Akt signal directly regulates the maintenance of regenerative cells.

In addition to the effect on macrophage recruitment, AS also impaired the recruitment of neutrophils (unpublished observation), indicating that the PI3Kγ signal affects the migration of myeloid cells. Although neutrophil-macrophage crosstalk in tissue repair is suggested (Tauzin et al., 2014), our previous study has shown that neutrophils are not necessary for supporting regenerative cell survival (Hasegawa et al., 2017).

A limitation of this study is that the target cells of AS were still unclear due to technical limitations such as cell type-specific gene knockdowns. Whole-mount in situ hybridization analysis (data not shown) and RNA sequencing data (Hasegawa et al., 2017; Rougeot et al., 2019) showed that *pik3cg* is expressed in variety of tissues, including macrophages and fin fold tissue. Therefore, it was difficult to precisely determine the AS target cells. Studies in mice have suggested that PI3Kγ regulates macrophage motility (Hirsch et al., 2000; Kaneda et al., 2016). Therefore, it is most likely that AS targets the PI3Kγ in the macrophage to regulate their recruitment to the injured site.

Considering the injury-dependent accumulation of macrophages at the injured site, tissue injury may produce a factor that influences the PI3Kγ activation. Chemokines from the injured tissue could function upstream of PI3Kγ to regulate macrophage recruitment. CCL5 is suggested to play a key role in activating macrophage chemotaxis (Barberis et al., 2009). In addition, PI3Kγ is reported to be activated by G protein couple receptor and P110γ during cellular chemotaxis in response to inflammation (Hirsch et al., 2010; Vadas et al., 2013). More recently, it has been reported that the neuregulin 1 (NRG1) secretion in the injured fin fold is required for macrophage recruitment (Laplace-Builhé et al., 2021). However, the mechanism by which the wounded tissue attracts macrophages remains unanswered.

In contrast to the role of PI3Kγ for macrophage recruitment, we showed that Akt is not involved in macrophage recruitment to injured site. Although Akt is one of well-known mediators of PI3K signal (Bondeva et al., 1998), it is likely that Akt is not the mediator of PI3Kγ for macrophage recruitment. Instead, an unknown component mediates the PI3Kγ signal to regulate macrophage migration. This is consistent with previous work showing that PI3Kγ is necessary for directed migration of neutrophils through phosphatidylinositol (3,4,5)P3-phosphatidylinositol(3,4)P2 (PI(3,4,5)P3-PI(3,4)P2) and Rac (Yoo et al., 2010).

caAkt-overexpression experiment indicated that Akt supports cell survival irrespective of macrophage recruitment, showing that it functions after macrophage recruitment in the regenerative cells for their survival. This notion was supported by Akt phosphorylation in the injured site in response to tissue injury. Akt incorporated into the plasma membrane is activated by phosphorylation at Thr308 and Thr473 (Vara et al., 2004). It is speculated that Akt in regenerative cells could be activated by a factor from the recruited macrophage (Hasegawa et al., 2015), although the entity of the surviving factor, which could be a protein or non-protein molecule (Yin et al., 2006; Sansbury et al., 2021; Serhan et al., 2012), is unknown.

ACKNOWLEDGMENTS

We thank Zebrafish International Resource Center (ZIRC) for providing *Tg(mpeg1:mCherry)* and the Drug Discovery Initiative of Tokyo University (DDI) for providing the chemical library. We are grateful to T. Ishitani for his generous gift of the *pTol2(hsp70l:mKO2)* plasmid. We thank the Open Facility Center for Life Science and Technology at the Tokyo Institute of Technology for sequencing and imaging support. This work was funded by the Grant-in-Aid for Scientific Research (B) (19H03232) and Challenging Exploratory Research (19K22417) to Atsushi Kawakami. Siyu Zhou was supported by the Tsubame Scholarship for Doctoral Students of the Tokyo Institute of Technology.

FUNDING INFORMATION

Grant-in-Aid for Scientific Research (B) (19H03232) and Challenging Exploratory Research (19K22417).

CONFLICT OF INTEREST

The authors have no conflicts of interest directly relevant to the content of this article.

ORCID

Atsushi Kawakami https://orcid.org/0000-0001-9461-6372

REFERENCES

Akieda, Y., Ogamino, S., Furuie, H., Ishitani, S., Akiyoshi, R., Nogami, J., Masuda, T., Shimizu, N., Ohkawa, Y., & Masuda, T. (2019). Cell competition corrects noisy Wnt morphogen gradients to achieve robust patterning in the zebrafish embryo. *Nature Communications*, *10*, 4710. https://doi.org/10.1038/s41467-019-12609-4

Aztekin, C., Hiscock, T. W., Butler, R., De Jesús Andino, F., Robert, J., Gurdon, J. B., & Jullien, J. (2020). The myeloid lineage is required for the emergence of a regeneration-permissive environment following *Xenopus* tail amputation. *Development*, *147*, dev185496. https://doi.org/10.1242/dev.185496

Barberis, L., Pasquali, C., Bertschy-Meier, D., Cuccurullo, A., Costa, C., Ambrogio, C., Vilbois, F., Chiarle, R., Wymann, M., Altruda, F., Rommel, C., & Hirsch, E. (2009). Leukocyte transmigration is modulated by chemokine-mediated PI3Kγ-dependent phosphorylation of vimentin. *European Journal of Immunology*, *39*, 1136–1146. https://doi.org/10.1002/eji.200838884

Bondeva, T., Pirola, L., Bulgarelli-Leva, G., Rubio, I., Wetzker, R., & Wymann, M. P. (1998). Bifurcation of lipid and protein kinase signals

of PI3Kγ to the protein kinases PKB and MAPK. *Science*, *282*, 293–296. https://doi.org/10.1126/science.282.5387.293

Camps, M., Rückle, T., Ji, H., Ardissone, V., Rintelen, F., Shaw, J., Ferrandi, C., Chabert, C., Gillieron, C., Françon, B., Martin, T., Gretener, D., Perrin, D., Leroy, D., Vitte, P.-A., Hirsch, E., Wymann, M. P., Cirillo, R., Schwarz, M. K., & Rommel, C. (2005). Blockade of PI3Kγ suppresses joint inflammation and damage in mouse models of rheumatoid arthritis. *Nature Medicine*, *11*, 936–943. https://doi.org/10.1038/nm1284

Ellett, F., Pase, L., Hayman, J. W., Andrianopoulos, A., & Lieschke, G. J. (2011). mpeg1 promoter transgenes direct macrophage-lineage expression in zebrafish. *Blood*, *117*, e49–e56. https://doi.org/10.1182/blood-2010-10-314120

Frank, T., Tuppi, M., Hugle, M., Dötsch, V., van Wijk, S. J., & Fulda, S. (2019). Cell cycle arrest in mitosis promotes interferon-induced necroptosis. *Cell Death and Differentiation*, *26*, 2046–2060. https://doi.org/10.1038/s41418-019-0298-5

Franke, T. F., Hornik, C. P., Segev, L., Shostak, G. A., & Sugimoto, C. (2003). PI3K/Akt and apoptosis: Size matters. *Oncogene*, *22*, 8983–8998. https://doi.org/10.1038/sj.onc.1207115

Geary, T. G., Mackenzie, C. D., & Silber, S. A. (2019). Flubendazole as a macrofilaricide: History and background. *PLoS Neglected Tropical Diseases*, *13*, e0006436. https://doi.org/10.1371/journal.pntd.0006436

Godwin, J. W., Pinto, A. R., & Rosenthal, N. A. (2013). Macrophages are required for adult salamander limb regeneration. *Proceedings of the National Academy of Sciences USA*, *110*, 9415–9420. https://doi.org/10.1073/pnas.1300290110

Han, Y., Chen, A., Umansky, K. B., Oonk, K. A., Choi, W.-Y., Dickson, A. L., Ou, J., Cigliola, V., Yifa, O., Cao, J., Tornini, V. A., Cox, B. D., Tzahor, E., & Poss, K. D. (2019). Vitamin D stimulates cardiomyocyte proliferation and controls organ size and regeneration in zebrafish. *Developmental Cell*, *48*, 853–863. https://doi.org/10.1016/j.devcel.2019.01.001

Hasegawa, T., Hall, C. J., Crosier, P. S., Abe, G., Kawakami, K., Kudo, A., & Kawakami, A. (2017). Transient inflammatory response mediated by interleukin-1β is required for proper regeneration in zebrafish fin fold. *eLife*, *6*, e22716. https://doi.org/10.7554/eLife.22716.001

Hasegawa, T., Nakajima, T., Ishida, T., Kudo, A., & Kawakami, A. (2015). A diffusible signal derived from hematopoietic cells supports the survival and proliferation of regenerative cells during zebrafish fin fold regeneration. *Developmental Biology*, *399*, 80–90. https://doi.org/10.1016/j.ydbio.2014.12.015

Hirsch, E., Katanaev, V. L., Garlanda, C., Azzolino, O., Pirola, L., Silengo, L., Sozzani, S., Mantovani, A., Altruda, F., & Wymann, M. P. (2000). Central role for G protein-coupled phosphoinositide 3-kinase gamma in inflammation. *Science*, *287*, 1049–1053. https://doi.org/10.1126/science.287.5455.1049

Ishida, T., Nakajima, T., Kudo, A., & Kawakami, A. (2010). Phosphorylation of Junb family proteins by the Jun N-terminal kinase supports tissue regeneration in zebrafish. *Developmental Biology*, *340*, 468–479. https://doi.org/10.1016/j.ydbio.2010.01.036

Kaneda, M. M., Messer, K. S., Ralainirina, N., Li, H., Leem, C. J., Gorjestani, S., Woo, G., Nguyen, A. V., Figueiredo, C. C., Foubert, P., Schmid, M. C., Pink, M., Winkler, D. G., Rausch, M., Palombella, V. J., Kutok, J., McGovern, K., Frazer, K. A., Wu, X., … Varner, J. A. (2016). PI3Kγ is a molecular switch that controls immune suppression. *Nature*, *539*, 437–442. https://doi.org/10.1038/nature19834

Kawakami, A. (2010). Stem cell system in tissue regeneration in fish. *Development, Growth & Differentiation*, *52*, 77–87. https://doi.org/10.1111/j.1440-169X.2009.01138.x

Kawakami, A., Fukazawa, T., & Takeda, H. (2004). Early fin primordia of zebrafish larvae regenerate by a similar growth control mechanism with adult regeneration. *Developmental Dynamics*, *231*, 693–699. https://doi.org/10.1002/dvdy.20181

Kohn, A. D., Summers, S. A., Birnbaum, M. J., & Roth, R. A. (1996). Expression of a constitutively active Akt Ser/Thr kinase in 3T3-L1 adipocytes stimulates glucose uptake and glucose transporter 4 translocation. *Journal of Biological Chemistry*, *271*, 31372–31378. https://doi.org/10.1074/jbc.271.49.31372

Laplace-Builhé, B., Barthelaix, A., Assou, S., Bohaud, C., Pratlong, M., Severac, D., Tejedor, G., Luz-Crawford, P., Nguyen-Chi, M., Mathieu, M., Jorgensen, C., & Djouad, F. (2021). NRG1/ErbB signalling controls the dialogue between macrophages and neural crest-derived cells during zebrafish fin regeneration. *Nature Communications*, *12*, 6336. https://doi.org/10.1038/s41467-021-26422-5

Longo, M., Zanoncelli, S., Colombo, P. A., Harhay, M. O., Scandale, I., Mackenzie, C., Geary, T., Madrill, N., & Mazué, G. (2013). Effects of the benzimidazole anthelmintic drug flubendazole on rat embryos in vitro. *Reproductive Toxicology*, *36*, 78–87. https://doi.org/10.1016/j.reprotox.2012.12.004

Longo, M., Zanoncelli, S., Messina, M., Scandale, I., Mackenzie, C., Geary, T., Marsh, K., Lindley, D., & Mazué, G. (2014). In vivo preliminary investigations of the effects of the benzimidazole anthelmintic drug flubendazole on rat embryos and fetuses. *Reproductive Toxicology*, *49*, 33–42. https://doi.org/10.1016/j.reprotox.2014.06.009

Mateus, R., Pereira, T., Sousa, S., de Lima, J. E., Pascoal, S., Saúde, L., & Jacinto, A. (2012). In vivo cell and tissue dynamics underlying zebrafish fin fold regeneration. *PLoS One*, *7*, e51766. https://doi.org/10.1371/journal.pone.0051766

Mathew, L. K., Sengupta, S., Kawakami, A., Andreasen, E. A., Löhr, C. V., Loynes, C. A., Renshaw, S. A., Peterson, R. T., & Tanguay, R. L. (2007). Unraveling tissue regeneration pathways using chemical genetics. *Journal of Biological Chemistry*, *282*, 35202–35210. https://doi.org/10.1074/jbc.M706640200

Merighi, S., Mirandola, P., Varani, K., Gessi, S., Capitani, S., Leung, E., Baraldi, P. G., Tabrizi, M. A., & Borea, P. A. (2003). Pyrazolotriazolopyrimidine derivatives sensitize melanoma cells to the chemotherapic drugs: Taxol and vindesine. *Biochemical Pharmacology*, *66*, 739–748. https://doi.org/10.1016/S0006-2952(03)00400-3

Mishra, R., Sehring, I., Cederlund, M., Mulaw, M., & Weidinger, G. (2020). NF-κB signaling negatively regulates osteoblast dedifferentiation during zebrafish bone regeneration. *Developmental Cell*, *52*, 167–182. https://doi.org/10.1016/j.devcel.2019.11.016

Nakamura, H., Noh, J. Y., Itoh, K., Fukata, S., Miyauchi, A., Hamada, N., & Working Group of the Japan Thyroid Association for the Guideline of the Treatment of Graves' Disease. (2007). Comparison of methimazole and propylthiouracil in patients with hyperthyroidism caused by Graves' disease. *The Journal of Clinical Endocrinology & Metabolism*, *92*, 2157–2162. https://doi.org/10.1210/jc.2006-2135

Oppedal, D., & Goldsmith, M. I. (2010). A chemical screen to identify novel inhibitors of fin regeneration in zebrafish. *Zebrafish*, *7*, 53–60. https://doi.org/10.1089/zeb.2009.0633

Petrie, T. A., Strand, N. S., Tsung-Yang, C., Rabinowitz, J. S., & Moon, R. T. (2014). Macrophages modulate adult zebrafish tail fin regeneration. *Development*, *141*, 2581–2591. https://doi.org/10.1242/dev.098459

Poss, K. D. (2010). Advances in understanding tissue regenerative capacity and mechanisms in animals. *Nature Reviews Genetics*, *11*, 710–722. https://doi.org/10.1038/nrg2879

Poss, K. D., Keating, M. T., & Nechiporuk, A. (2003). Tales of regeneration in zebrafish. *Developmental Dynamics*, *226*, 202–210. https://doi.org/10.1002/dvdy.10220

Rojas-Muñoz, A., Rajadhyksha, S., Gilmour, D., van Bebber, F., Antos, C., Esteban, C. R., Nüsslein-Volhard, C., & Belmonte, J. C. I. (2009). ErbB2 and ErbB3 regulate amputation-induced proliferation and migration during vertebrate regeneration. *Developmental Biology*, *327*, 177–190. https://doi.org/10.1016/j.ydbio.2008.12.012

Rosania, G. R., Chang, Y.-T., Perez, O., Sutherlin, D., Dong, H., Lockhart, D. J., & Schultz, P. G. (2000). Myoseverin, a microtubule-

binding molecule with novel cellular effects. *Nature Biotechnology*, *18*, 304–308. https://doi.org/10.1038/73753

Rougeot, J., Torraca, V., Zakrzewska, A., Kanwal, Z., Jansen, H. J., Sommer, F., Spaink, H. P., & Meijer, A. H. (2019). RNAseq profiling of leukocyte populations in zebrafish larvae reveals a cxcl11 chemokine gene as a marker of macrophage polarization during mycobacterial infection. *Frontiers in Immunology*, *10*, 832. https://doi.org/10.3389/fimmu.2019.00832

Sakamoto, T., Kondo, K., Kashio, A., Suzukawa, K., & Yamasoba, T. (2007). Methimazole-induced cell death in rat olfactory receptor neurons occurs via apoptosis triggered through mitochondrial cytochrome c-mediated caspase-3 activation pathway. *Journal of Neuroscience Research*, *85*, 548–557. https://doi.org/10.1002/jnr.21155

Sansbury, B. E., Li, X., Wong, B., Riley, C. O., Shay, A. E., Nshimiyimana, R., Petasis, N. A., Serhan, C. N., & Spite, M. (2021). PCTR1 enhances repair and bacterial clearance in skin wounds. *The American Journal of Pathology*, *191*, 1049–1063. https://doi.org/10.1016/j.ajpath.2021.02.015

Serhan, C. N., Dalli, J., Karamnov, S., Choi, A., Park, C.-K., Xu, Z.-Z., Ji, R.-R., Zhu, M., & Petasis, N. A. (2012). Macrophage proresolving mediator maresin 1 stimulates tissue regeneration and controls pain. *The FASEB Journal*, *26*, 1755–1765. https://doi.org/10.1096/fj.11-201442

Shibata, E., Ando, K., Murase, E., & Kawakami, A. (2018). Heterogeneous fates and dynamic rearrangement of regenerative epidermis-derived cells during zebrafish fin regeneration. *Development*, *145*, dev162016. https://doi.org/10.1242/dev.162016

Shibata, E., Yokota, Y., Horita, N., Kudo, A., Abe, G., Kawakami, K., & Kawakami, A. (2016). Fgf signalling controls diverse aspects of fin regeneration. *Development*, *143*, 2920–2929. https://doi.org/10.1242/dev.140699

Simões, F. C., Cahill, T. J., Kenyon, A., Gavriouchkina, D., Vieira, J. M., Sun, X., Pezzolla, D., Ravaud, C., Masmanian, E., Weinberger, M., Mayes, S., Lemieux, M. E., Barnette, D. N., Gunadasa-Rohling, M., Williams, R. M., Greaves, D. R., Trinh, L. A., Fraser, S. E., Dallas, S. L., … Riley, P. R. (2020). Macrophages directly contribute collagen to scar formation during zebrafish heart regeneration and mouse heart repair. *Nature Communications*, *11*, 600. https://doi.org/10.1038/s41467-019-14263-2

Stainier, D. Y., Weinstein, B. M., Detrich, H. W., Zon, L. I., & Fishman, M. C. (1995). Cloche, an early acting zebrafish gene, is required by both the endothelial and hematopoietic lineages. *Development*, *121*, 3141–3150. https://doi.org/10.1242/dev.121.10.3141

Tauzin, S., Starnes, T. W., Becker, F. B., Lam, P., & Huttenlocher, A. (2014). Redox and Src family kinase signaling control leukocyte wound attraction and neutrophil reverse migration. *Journal of Cell Biology*, *207*, 589–598. https://doi.org/10.1083/jcb.201408090

Todd, P. A., & Karen, L. G. (1990). Simvastatin. A review of its pharmacological properties and therapeutic potential in hypercholesterolaemia. *Drugs*, *40*, 583–607. https://doi.org/10.2165/00003495-199040040-00007

Tsarouchas, T. M., Wehner, D., Cavone, L., Munir, T., Keatinge, M., Lambertus, M., Underhill, A., Barrett, T., Kassapis, E., Ogryzko, N., Feng, Y., van Ham, T. J., Becker, T., Becker, C. G., & Becker, C. G. (2018). Dynamic control of proinflammatory cytokines Il-1β and Tnf-α by macrophages in zebrafish spinal cord regeneration. *Nature Communications*, *9*, 4670. https://doi.org/10.1038/s41467-018-07036-w

Um, J., Jung, D.-W., & Williams, D. R. (2017). Lessons from the swamp: Developing small molecules that confer salamander muscle cellularization in mammals. *Clinical and Translational Medicine*, *6*, e13. https://doi.org/10.1186/s40169-017-0143-8

Vadas, O., Dbouk, H. A., Shymanets, A., Perisic, O., Burke, J. E., Abi Saab, W. F., Khalil, B. D., Harteneck, C., Bresnick, A. R., Nürnberg, B., Backer, J. M., & Williams, R. L. (2013). Molecular determinants of PI3Kγ-mediated activation downstream of G-protein–coupled receptors (GPCRs). *Proceedings of the National Academy of Sciences USA*, *110*, 18862–18867. https://doi.org/10.1073/pnas.1304801110

Vara, J. Á. F., Casado, E., de Castro, J., Cejas, P., Belda-Iniesta, C., & González-Barón, M. (2004). PI3K/Akt signalling pathway and cancer. *Cancer Treatment Reviews*, *30*, 193–204. https://doi.org/10.1016/j.ctrv.2003.07.007

Wehner, D., & Weidinger, G. (2015). Signaling networks organizing regenerative growth of the zebrafish fin. *Trends in Genetics*, *31*, 336–343. https://doi.org/10.1016/j.tig.2015.03.012

Yin, Y., Henzl, M. T., Lorber, B., Nakazawa, T., Thomas, T. T., Jiang, F., Langer, R., & Benowitz, L. I. (2006). Oncomodulin is a macrophage-derived signal for axon regeneration in retinal ganglion cells. *Nature Neuroscience*, *9*, 843–852. https://doi.org/10.1038/nn1701

Yoo, S. K., Deng, Q., Cavnar, P. J., Wu, Y. I., Hahn, K. M., & Huttenlocher, A. (2010). Differential regulation of protrusion and polarity by PI (3) K during neutrophil motility in live zebrafish. *Developmental Cell*, *18*, 226–236. https://doi.org/10.1016/j.devcel.2009.11.015

Yoshinari, N., & Kawakami, A. (2011). Mature and juvenile tissue models of regeneration in small fish species. *The Biological Bulletin*, *221*, 62–78. https://doi.org/10.1086/BBLv221n1p62

Yun, M. H., Davaapil, H., & Brockes, J. P. (2015). Recurrent turnover of senescent cells during regeneration of a complex structure. *eLife*, *4*, e05505. https://doi.org/10.7554/eLife.05505.001

SUPPORTING INFORMATION

Additional supporting information can be found online in the Supporting Information section at the end of this article.

How to cite this article: Zhou, S., Liu, Z., & Kawakami, A. (2022). A PI3Kγ signal regulates macrophage recruitment to injured tissue for regenerative cell survival. *Development, Growth & Differentiation*, *64*(8), 433–445. https://doi.org/10.1111/dgd.12809